Probing the π-Stacking Induced Molecular Aggregation in π-Conjugated Polymers, Oligomers, and Their Blends of *p*-Phenylenevinylenes

S. R. Amrutha and M. Jayakannan*

Chemical Sciences and Technology Division, National Institute for Interdisciplinary Science and Technology, Thiruvananthapuram-695019, Kerala, India

Received: September 14, 2007; In Final Form: October 31, 2007

The role of π-stack induced molecular aggregation on solution and solid-state luminescent properties was investigated for the tricyclodecane substituted bulky (*p*-phenylenevinylene)s (BTCD-60, with 60% bulky group), oligophenylenevinylenes (MEH-OPV and BTCD-OPV)s, and their polymer-oligomer binary blends. The natures of the solvent, concentration, solvent combinations (good or bad), and temperature were employed as stimuli to probe the origin of the molecular aggregates in bulky conducting polymers. Absorption, photoluminescence (PL), and time-resolved fluorescence spectroscopic techniques were employed as tools to trace aggregation in solvents such as toluene, tetrahydrofuran (THF), THF and methanol, or THF and water as well as in the solid state. The absorbance spectra of poly(2-methoxy-5-(2-ethylhexyloxy))-1,4-phenylenevinylene (MEH-PPV**)** and BTCD-60 indicated that the films obtained from polymers that were dissolved in aromatic solvents such as toluene were found to possess more π-stacking as compared to that of films obtained from a good solvent such as THF. The solid-state emission spectrum of BTCD-60 was found to show almost a 5−6 times enhancement in PL intensity as compared to that of MEH-PPV. Concentration dependent excitation spectra of the polymers confirmed the presence of aggregated polymer chains in MEH-PPV, which is the main reason for the quenching of luminescence intensity in the polymer. Solvent induced aggregation studies of polymers in THF and methanol mixture further supports the existence of strong aggregation in MEH-PPV as compared to that of bulky BTCD-60. Variable temperature absorption studies confirmed the reversibility of molecular aggregation on heating/cooling cycles, and the extent of aggregation was found more in MEH-PPV chains as compared to that of BTCD-60. MEH-PPV/OPV binary blends were prepared in the entire composition range from 0 to 100% via solution blending techniques. Through selective PL excitation techniques, the effect of oligomer-to-polymer energy transfer and also luminescent enhancement in MEH-PPV via interchain separation were investigated. Both the energy transfer and the interchain separation were found to be more effective on the enhancement of luminescence properties in the BTCD blends as compared to that of MEH blends. Time-resolved fluorescence studies confirmed the existence of two types of species corresponding to the free and aggregated chains in the polymer matrix with lifetimes in the range of 0.5−2.0 ns. In the present investigation, we have successfully shown that the molecular aggregation of the π-conjugated polymers, oligomers, and their binary blends can be controlled via suitable bulky substitution to tune their emission properties in solution as well as in the solid state.

Introduction

Poly(*p*-phenylenevinylene)s (PPVs) and their derivatives have attained wide interest because of their applications in optoelectronic devices such as light emitting diodes and photovoltaic cells.[1−6] Color-tuning via suitable electron rich or deficient anchoring units[7−13] and good solubility in common organic solvents for better processing in devices are some of the added advantages of the PPV and its copolymers compared to other conjugated polymers.[14−20] In general, almost all the polymeric emitters are able to form excimers; however, many of them fail as highly luminescent emitters. The conjugated polymer chains have a very high tendency for aromatic $-\pi-\pi$-interactions, which lead to the formation of weakly emissive aggregated species predominantly in the solid state (in films).[21−30] These molecular aggregates are normally lower energy non-emissive species in which the excitation energy of the highly luminescent excimers becomes trapped during the radiative emission processes (photoluminescence and electroluminescence). Therefore, many highly luminescent π-conjugated polymers in solution were found to be weakly emissive in the film over a long period of storage in molecular electronics.

Now, it has been realized that the control of π-stack induced molecular aggregation in the polymer chain is an important task in the development of highly emissive conjugated polymers and also in making ideal polymer luminescent optoelectronic devices. Various synthetic approaches have been reported for controlling molecular aggregation in the conjugated polymers, which include the incorporation of *cis*-vinylene linkages in the polymer backbone,[31−36] polymer blends,[37−40] and the introduction of bulky anchoring groups,[41−45] etc. The meta substitution in the conjugated backbone was successful in improving the solubility and prevention of aggregation in the polymer chain. However, the HOMO−LUMO energies and emission color of the confined structures were found to be completely different from that of the parent chain, which is undesirable. The control

* Corresponding author. Present address: Department of Chemistry, Indian Institute of Science Education and Research (IISER), 900 NCL Innovation Park, Dr. Homi Bhabha Road, Pune 411008, India. E-mail: jayakannan@iiserpune.ac.in. Fax: 0091-20-25898022.

10.1021/jp077404z CCC: $40.75
Published on Web 01/08/2008

of molecular aggregation through interchain separation via bulky anchoring groups was found to be very attractive since one can easily control the molecular aggregation through space without disturbing the electronic/device properties of the parent polymer. Attempts have been reported for bulky PPVs using alkoxy units of cyclohexyl,[46,47] adamantane,[48,49] and cholestanyl rings;[50,51] aryloxy units of phenyl,[52] biphenyl,[53] and naphthyl;[54] and inorganic pendants such as silyl[55] and silsesquioxane[56,57] to control the molecular aggregation in the solid state. The substitution of bulky anchoring groups has additional advantages in that they also enhance the glass transition temperature (T_g) of PPV; a high T_g is an important parameter for long operating lifetimes of devices.[58]

In our effort to control the molecular aggregation in π-conjugated polymers, we have recently reported a new series of soluble and processable bulky PPVs bearing tricyclodecanemethylene (TCD) units as the pendant group.[59,60] The preliminary investigation suggested that the introduction of TCD units in the PPV backbone reduces the molecular aggregation and enhances the solution and solid-state photoluminescence characteristics.[59] Many parameters of PPV chains such as liquid crystallinity, solubility, and a high glass transition temperature (from 80 to 200 °C) were fine-tuned by varying the amount as well as mono- or bis-TCD substitution in the backbone.[60] It is surprising to notice that the reports on the bulky π-conjugated polymers have mostly focused on the structural parameters, and so far, not much effort has been paid to trace the aggregation behavior of these emerging bulky conjugated materials. This is partially due to the poor solubility of the efficient bulky PPVs such as adamantane and cholestanyl rings[48−51] in common organic solvents that hampered the application of spectroscopic techniques to study the aggregation properties in solution. Therefore, it is very important to carry out systematic spectroscopic studies to probe the origin of the molecular aggregates in bulky conducting polymers, which will provide valuable information for the future development of new highly luminescent materials.

The present investigation investigated the molecular aggregation properties of soluble TCD substituted bulky PPVs in combination with the well-studied poly(2-methoxy-5-ethylhexyloxy)-1,4-phenylenevinylene (MEH-PPV). A random copolymer of MEH-PPV with 60% TCD content was chosen for the previous purpose due to its high solubility, good molecular weight, and the fact that it bears photophysical properties that are equal to its partially soluble bulky TCD-PPV homopolymer.[59,60] Two oligo(phenylenevinylene)s (OPV)s bearing either (methoxy-ethylhexyloxy) (MEH) or TCD units that are structurally identical were also synthesized and utilized as model compounds for the aggregation studies. Absorption and photoluminescence (PL) spectroscopic techniques were employed as tools to trace the aggregation properties of these materials in solvents such as toluene, tetrahydrofuran (THF), THF and methanol, or THF and water combinations as well as in the solid state. Furthermore, the effect of bulky TCD anchoring units on the luminescence properties of the PPV backbone was also investigated for MEH-PPV and OPV binary blends. The composition of the MEH-PPV and OPVs was varied from 0 to 100%. Through selective PL excitation, both the effect of the oligomer-to-polymer energy transfer and also the luminescent enhancement in MEH-PPV via interchain separation were investigated. Time-resolved fluorescence decay measurements were also carried out to study the luminescent decay lifetime of bulky polymers, oligomers, and their binary blends. We have successfully shown that molecular aggregation of the π-conjugated polymers, oligomers, and their binary blends can be controlled via suitable bulky substitution to tune their emission properties in solution as well as in the solid state.

Experimental Procedures

Materials. TCD was donated by Celanese Chemicals Co., and fluorescence standards rhodamine 6G and quinine sulfate were purchased from Aldrich Chemicals and used without further purification. 1-Methoxy-4-(2-ethylhexyloxy)benzene, 1,4-bis(1,8-tricyclodecanemethyleneoxy)benzene, 1,4-bis(bromomethyl)-2-methyloxy-5-(2-ethylhexyloxy)benzene, 1,4-bis(bromomethyl)-2,5-di(1,8-tricyclodecanemethyleneoxy)benzene, MEH-PPV (M_n = 20 300 and M_w = 70 100), and poly[(2-methoxy-5-(2-ethylhexyloxy))-1,4-phenylenevinylene-*co*-(2,5-bis(1,8-tricyclodecanemethyleneoxy)-1,4-phenylenevinylene] (BTCD-60) (with 60% TCD content, M_n = 9300 and M_w = 23 900) were synthesized as reported earlier.[59,60]

Instrumentation. ^{1}H and ^{13}C NMR spectra of the samples were recorded using a 300 MHz Bruker NMR spectrophotometer in $CDCl_3$, containing small amounts of TMS as an internal standard. Infrared spectra of the samples were recorded with a PekinElmer Fourier transform infrared spectrophotometer in the solid state. The purity of the monomers, model compounds, etc. were determined using JEOL JSM600 fast atom bombardment (FAB) high-resolution mass spectrometry instrument. Elemental analysis of the model compounds and polymers was carried out using an Elementar Vario EL-III CHN analyzer. Cyclic voltammetry (CV) measurements were carried out with the model 1100A electrochemical analyzer (CH Instruments). This instrument is a conventional three electrode cell that uses a Pt button working electrode of 2 mm in diameter, Pt wire as the counter electrode, and Ag/AgCl as the reference electrode. The experiment was carried out using 0.1 M Bu_4NPF_6 as the supporting electrolyte under nitrogen gas protection at a scan rate of 0.1 V/s at 25 °C. The measurements were taken by making solutions in spectroscopic grade CH_2Cl_2 for the OPVs and preparing thin films on the Pt electrode surface for the polymers. For the photophysical studies, all the solvents were purified according to the standard procedures prior to use. The samples were completely dissolved by ultrasonication, and the homogeneous solutions thus obtained were used for further studies. The absorption and emission studies were performed using a PerkinElmer Lambda 35 UV−vis spectrophotometer and a Spex-Fluorolog DM3000F spectrofluorometer with a double grating 0.22 m Spex 1680 monochromator and a 450 W Xe lamp as the excitation source using the front-face mode. For the solid-state spectra, polymer thin films (10−100 μM) were casted from THF solution on glass substrates. The quantum yields of the PPVs and OPVs were determined using rhodamine 6G in water (ϕ = 0.95) and quinine sulfate in 0.1 M H_2SO_4 (ϕ = 0.546) as standards, respectively. The solvent induced aggregation studies were performed using methanol (MeOH) and water as non-solvents, respectively, for PPVs and OPVs and by making different solvent/non-solvent combinations. The absorbance or optical density (OD) of the solutions was maintained at 0.1 for the photophysical studies. The stock solution was prepared by dissolving the polymer or oligomer in THF, and various combinations of THF and methanol/water samples were prepared by maintaining the absorbance at ≈0.1. Temperature dependent absorbance studies were performed in a THF/methanol or a THF/water mixture, and heating and cooling were performed with the help of a PerkinElmer PTP-1 Peltier cooling system. The fluorescence lifetime was measured using an IBH FlouroCube time-correlated picosecond single-

photon counting system (TCSPC). Solutions and films were excited with a pulsed diode laser (401 nm < 100 ps pulse duration) with a repetition rate of 1 MHz. The detection system consisted of a microchannel plate photomultiplier (5000U-09B, Hamamatsu) with a 38.6 ps response time coupled to a monochromator (5000 M) and TCSPC electronics (DataStation Hub including Hub-NL, NanoLED controller, and preinstalled fluorescence measurement and analysis studio (FMAS) software). The fluorescence lifetime values were determined by deconvoluting the data with exponential decay using DAS6 decay analysis software. The quality of the fit was judged by the fitting parameters such as $\chi^2 < 1$ as well as visual inspection of the residuals.

Synthesis of Bulky Oligo Phenylenevinylenes. The procedure is described in detail for 1,4-bis(1,8-tricyclodecanemethyleneoxy)-2,5-distyrylbenzene (BTCD-OPV). 1,4-Bis(bromomethyl)-2,5-di(1,8-tricyclodecanemethyleneoxy)benzene (2.00 g, 3.4 mmol) and triethyl phosphite (1.13 g, 6.8 mmol) were heated to 140−150 °C for 12 h under nitrogen atmosphere. Excess triethyl phosphite was removed by vacuum distillation to obtain the ylide 1,4-bis(tricyclodecanemethyleneoxy)-2,5-xylenetetraethyldiphosphonate as a white solid. ^{1}H NMR ($CDCl_3$) δ: 6.88 ppm (t, 2H, Ar−H), 4.06 ppm (m, 8H, -PO-OCH_2), 3.68 ppm (m, 4H, Ar-OCH_2), 3.24 ppm (m, 4H, Ar-CH_2P), 1.69−1.21 ppm (m, 42H, aliphatic). FTIR (cm^{-1}): 3445, 2947, 2868, 1681, 1509, 1474, 1415, 1392, 1305, 1245, 1210, 1163, 1094, 1048, 1029, 964, 894, 875, 831, 782, 729, 529 cm^{-1}. To the previous crude product (1.10 g, 1.6 mmol) in 50 mL of dry THF, benzaldehyde (0.41 g, 3.9 mmol) and potassium tert-butoxide (7 mL, 1 M THF) were added, and the contents were stirred under nitrogen atmosphere for 12 h at 30 °C. This solution was poured into methanol, and the yellow solid was filtered and purified by passing through silica gel column using ethyl acetate and hexane (1:20 v/v) as the eluent. Yield = 35%, mp = 225−226 °C. ^{1}H NMR ($CDCl_3$) δ: 7.53−6.97 ppm (m, 16H, Ar-H and vinylic H), 3.80−3.67 ppm (m, 4H, Ar-OCH_2), 2.41−0.98 ppm (m, 30H, cyclic-H). ^{13}C NMR ($CDCl_3$) δ: 151.3, 138.1, 129.0, 128.7, 127.4, 126.5, 123.8, 111.4 (Ar-C), 73.7 (Ar-OCH_3 + Ar-OCH_2), 45.7, 45.3, 44.0, 41.3, 40.3, 34.8, 29.7, 29.1, 28.0, 27.0, and 26.5 ppm (cyclic-C) FTIR (cm^{-1}): 3340, 2923, 2851, 1593, 1418, 1187, 1113, 1015, 965 (HC═CH, trans), 874 (HC═CH, cis), 869, 746, 683 cm^{-1}. HRMS (M_w: 610.9): m/z = 610.4 (M^+). Anal. calcd for $C_{44}H_{50}O_2$: C, 86.51; H, 8.25; Found C, 86.83; H, 8.03.

Similarly, 1-(methoxy)-4-(2-ethylhexyloxy)-2,5-distyrylbenzene (MEH-OPV) was prepared by starting from 1,4-bis(bromomethyl)-2-methoxy-5-(2-ethylhexyloxy)benzene, and then following the Wittig reaction conditions by treating with benzaldehyde as described for BTCD-OPV. Yield = 39%, mp = 53−54 °C. ^{1}H NMR ($CDCl_3$) δ: 7.50−7.06 ppm (m, 16H, Ar-H and vinylic H), 3.90−3.88 ppm (m, 2H, Ar-OCH_2), 3.86 ppm (s, 3H, Ar-OCH_3), 1.75−0.82 ppm (m, 15H, aliphatic). ^{13}C NMR ($CDCl_3$) δ: 151.4, 138.0, 128.9, 127.4, 126.9, 123.5, 110.3, 109.2 (Ar-C), 71.8 (Ar-OCH_2), 56.4 (Ar-OCH_3), 39.8, 30.9, 29.7, 29.3, 24.2, 23.1, 14.1, 11.3 ppm (cyclic-C) FTIR (cm^{-1}): 3340, 2923, 2857, 1739, 1591, 1495, 1459, 1410, 1256, 1201, 1038, 960 (HC═CH, trans), 875 (HC═CH, cis), 866, 839, 798, 749 cm^{-1}. HRMS (M_w: 440.6): m/z = 440.3 (M^+). Anal. calcd for $C_{31}H_{36}O_2$: C, 84.50; H, 8.24. Found C, 84.15; H, 8.52.

Synthesis of Binary Blends. The polymer-oligomer binary blends were prepared as follows. A filtered stock solution of MEH-PPV (2.8 mg in 10 mL) in THF and BTCD-OPV or MEH-OPV (50 mg in 10 mL) in THF were mixed at various ratios (see table in the Supporting Information) to obtain the OPV amount as 15, 30, 40, 55, 80, 90, and 95 wt % in the blend solution. The blend solution was stirred under ultrasonic radiation for 5−10 min prior to being cast on glass substrates. The films were dried and stored at room temperature to protect them from light.

Results and Discussion

MEH-PPV and BTCD-60 were prepared via the Gilch route from their respective bis-bromomethylated monomers using potassium tert-butoxide as the base catalyst at 30 °C in THF. In BTCD-60, the number 60 indicates the amount of bis-TCD units incorporated in the copolymer, which was determined by ^{1}H NMR techniques.[59,60] Structurally similar model compounds MEH-OPV and BTCD−OPV were synthesized by reacting the bis-ylides of the bis-bromomethylated monomers with benzaldehyde under Wittig reaction conditions. The structures of the polymers and oligomers are shown in Figure 1. The thermal stability of the polymers and oligomers was characterized by thermogravimetric analysis (TGA), and the results indicated that all compounds were highly stable up to ∼300 °C. The thermal degradation temperature of the polymers and oligomers for 10 wt % loss is given in Table 1, and the results indicate that the polymers and their structurally similar model compounds have a very high thermal stability for higher temperature applications. However, the thermal stability of these PPV polymers and derivatives was much lower than that of other conjugated polymers such as polyaniline, polypyrrole, and polythiophenes, etc.[17,61] Other thermal properties such as T_g, T_m, and T_c were analyzed by differential scanning calorimetry (DSC), and no melting or crystallization peaks in the heating and the cooling cycles occurred. The polymers MEH-PPV and BTCD-60 showed only glass transition temperatures at 78 and 143 °C, respectively. The higher T_g values for BTCD-60 confirmed the high rigidity of the BTCD-60 polymer backbone as a result of bulky TCD substitution. The effect of bulky substitution was again confirmed by the increase in the melting temperature (225−226 °C) of the bulky model compound (BTCD-OPV) as compared to its non-bulky counterpart (MEH-OPV). DSC and polarizing light microscopic (PLM) studies revealed that MEH-OPV was highly amorphous, whereas BTCD-OPV was obtained as a thermotropic liquid crystalline material (see Supporting Information). Detailed syntheses, structural characterization (by NMR and FTIR), molecular weight, and thermal analysis of the polymers and model compounds have been reported elsewhere.[59,60] In the present investigation, more effort has been paid to understanding the molecular aggregation properties of these new classes of bulky π-conjugated materials.

Photophysical Properties. The photophysical properties (absorption and emission) of the polymers were studied in solution as well as in the solid state (in film). The absorption and emission spectra of the polymers were recorded in THF and toluene to study the influence of solvents on the polymer structure (see Figure 2a). The absorption spectra of both polymers showed a 6−7 nm red shift in toluene as compared to that in THF (see Table 1). This is due to the fact that aromatic hydrocarbon solvents solvate the PPV backbone in such a way as to adopt closer chain interactions via π-stacking that account for the red shift.[22,62] The emission spectra of the polymers were recorded for 0.1 OD solutions in THF and toluene. The emission spectra were almost identical even though there was a slight difference in the absorption maxima for the polymer solutions in THF and toluene. The solution quantum yields were determined using rhodamine 6G in water as the standard (ϕ = 0.95), and the values were obtained in the range of 0.23−0.28

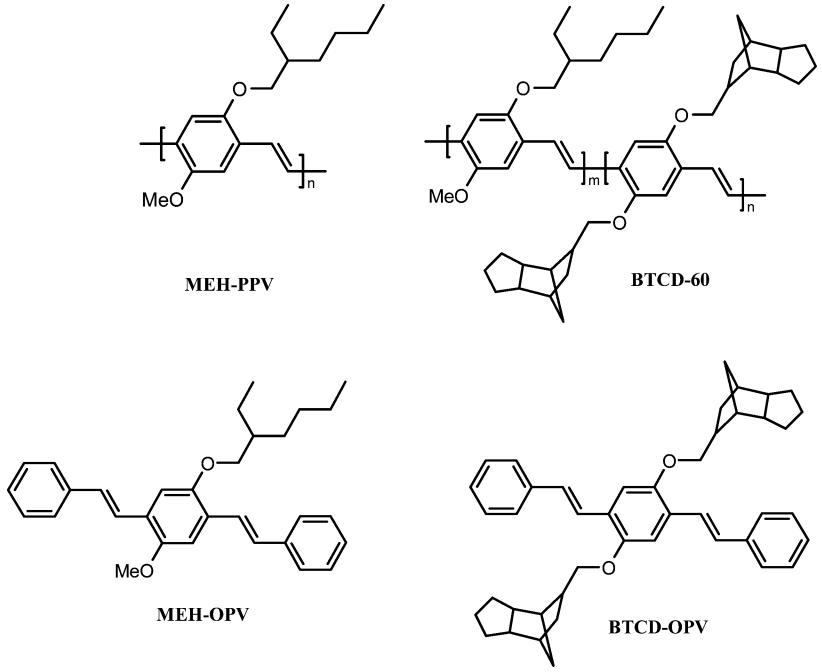

Figure 1. Structure of the polymers (MEH-PPV and bulky TCD-PPV) and oligomers (MEH-OPV and BTCD-OPV).

TABLE 1: Photophysical, Thermal, and Electrochemical Properties of Polymers and Oligomers

	in soln (nm)[a]			in film (nm)[b]					E_{ox}[c] (V)	
sample	λ_{abs}	λ_{em}	ϕ_{FL}[d]	λ_{abs}	λ_{em}	$PL_{intensity}$[e]	T_D[f] (°C)	T_g/T_m[g] (°C)	E_{onset}	E_p
MEH-PPV(THF)	489	549	0.28	502	584	4.3×10^5	322	78	0.52	1.50
MEH-PPV(toluene)	495	553	0.23	504	589	2.5×10^5				
BTCD-60(THF)	486	550	0.31	490	585	2.7×10^6	303	143	0.67	1.42
BTCD-60(toluene)	493	554	0.25	497	585	1.2×10^6				
MEH-OPV	389	433−475	0.53	394	525	$\phi = 0.27$[h]	298	53−54	0.93	1.4
BTCD-OPV	386	432−481	0.54	398	525	$\phi = 0.64$[h]	343	225−226	0.94	1.44

[a] Absorption and emission studies were performed in THF and toluene, and the excitation wavelength used was 480 nm for the polymers and 380 nm for the oligomers. [b] Excitation wavelength was 500 nm for polymers and 390 nm for the model compounds. [c] Onset and peak values of oxidation potential were obtained from the electrochemical measurements. [d] Solution quantum yields were determined using rhodamine 6G as a standard for the polymers (λ_{ex} = 480 nm) and quinine sulfate as the standard for the oligomers (λ_{ex} = 380 nm); the absorbance of solutions was maintained as 0.1 at the excitation wavelength. [e] Emission intensity of the polymers at the emission maxima. [f] Decomposition temperatures at 10% weight loss obtained from the TGA analysis. [g] Glass transition temperature of the polymers and melting point of the oligomers determined from the DSC analysis. BTCD-OPV was liquid crystalline. [h] Absolute solid-state quantum yield for the oligomers determined from the diffuse reflectance measurements.[60]

and 0.24−0.31 for MEH-PPV and BTCD-60, respectively (see Table 1). It can be clearly noticed that the emission quantum yield was less in toluene as compared to that of THF (see Table 1). This may be due to the partial π-stacking of the polymer chains in toluene as compared to that of THF, as noticed in their absorbance spectra. Thin polymer films were cast on a glass substrate from the polymer solution, and the OD of the films was obtained as 0.1 by adjusting the concentration of the polymer solution. The solid-state absorbance and emission spectra of films are shown in Figure 2b. The absorbance spectra of MEH-PPV and BTCD-60 films prepared from the toluene solution were almost identical and red shifted as compared to that of those films obtained from the THF solution. This suggests that the films cast from aromatic hydrocarbon solvents such as toluene possess more π-stacking as compared to that of the films from good solvent such as THF.[22,62]

Among the films produced from the THF solution, the absorption spectra of the BTCD-60 film is blue shifted by 15−20 nm as compared to the MEH-PPV films (compare plots a and b in Figure 2b). This indicates that interchain (or intrachain) interactions (π-stacking) are relatively weak in BTCD-60 as compared to MEH-PPV. This may be due to the strong steric hindrance induced by the TCD bulky unit. The optical band gap (E_g) of the polymers was calculated from the onset of the absorption spectra for all the solvent cast films. The values were obtained as 1.97 eV for toluene cast films (for both MEH-PPV and BTCD-60) and 2.08 and 2.15 eV for the films of MEH-PPV and BTCD-60, respectively, cast from the THF solution. The optical band gap clearly shows the existence of strong π-stacking in the films obtained from the aromatic solvent toluene as compared to the films cast from a good solvent such as THF. The solid-state emission spectra of the polymers have shown an interesting trend that the spectra of BTCD-60 was almost 5−6 times more enhanced in PL intensity than that of MEH-PPV. The emission intensity of the MEH-PPV films was very low for both films cast from toluene and THF (see emission plots a and a′ in Figure 2b) as compared to the BTCD-60 films. Among the two BTCD-60 films, the film obtained from the THF solution showed twice the PL intensity as compared to that of films obtained from the toluene solution (see emission plots b and b′ in Figure 2b). The comparison of absorbance and emission spectra of the films of BTCD-60 revealed that the less π-aggregated film (plot b in Figure 2b) showed a higher luminescence intensity as compared to that of more π-aggregated chains (plot b′ in Figure 2b). It evident that the molecular aggregation is a very strong phenomenon in PPV chains for

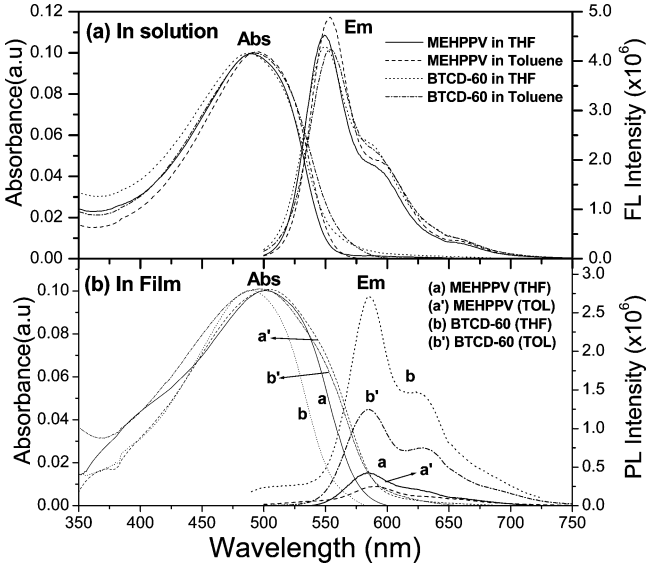

Figure 2. Absorption and emission spectra of MEH-PPV and BTCD-60 in solution (a) and film (b) (cast from THF and toluene solution) on glass substrate.

reduction in emission characteristics in both solutions as well as the films cast from their solution. The presence of a TCD bulky unit significantly hinders the π-stacking of the polymer backbone and enhances the solution quantum yield and PL intensity by almost 5−6 times in BTCD-60 as compared to that of MEH-PPV.

To trace the aggregated species at the excited state, the excitation spectra of the polymers were recorded at two different concentrations in THF (10^{-4} and 10^{-5} M^{-1}). The concentration dependent experiment was chosen since the polymer chains are closely packed at higher concentrations, which resembles the chain arrangements in the film.[63] The excitation spectra were also recorded for films; however, the spectra were very broad and contained less features and are not included in this discussion. The excitation spectra of MEH-PPV and BTCD-60 were collected at three different emission wavelengths (λ_{em} = 550, 590, and 660 nm) and are shown in Figure 3. At lower concentrations, the excitation spectra of MEH-PPV showed maxima at 470 nm with a shoulder at 340 nm at all three collected emission wavelengths. At higher concentrations, the intense peak was blue shifted by 70 nm and centered at ∼405 nm, corresponding to a strong interchain interaction and π-stacking in the concentrated solution.[63] Additionally, the excitation spectra were collected at higher emission wavelengths (collection at 590 and 660 nm), and the concentrated solution of MEH-PPV showed a new peak at 545 nm that was assigned to the aggregated polymer chains.[64] Interestingly, BTCD-60 showed almost identical excitation spectra irrespective of the concentration of the solution and collected emission wavelengths. It was confirmed that the MEH-PPV polymer chain underwent more π-stacking at higher concentration (similar to film), which results in quenching of the luminescence properties. The solid-state luminescence quantum yields of the model compounds MEH-OPV and BTCD-OPV were determined using a diffuse reflectance technique for excitation in the region of 330−360 nm using sodium salicylate as the standard (ϕ = 0.60).[60,65−68] It is very interesting to note that the quantum yield of the bulky TCD model compounds BTCD-OPV was obtained as 0.64, which was 2 times higher than that of MEH-OPV (ϕ = 0.27). This clearly demonstrates that the bulky TCD unit is a very efficient structure directing unit for highly luminescent π-conjugated materials. From the previously stated photophysical studies, it is evident that the bulky TCD unit increases the interchain distance in the polymer backbone, leading to reduction in the molecular aggregation for enhanced luminescence.

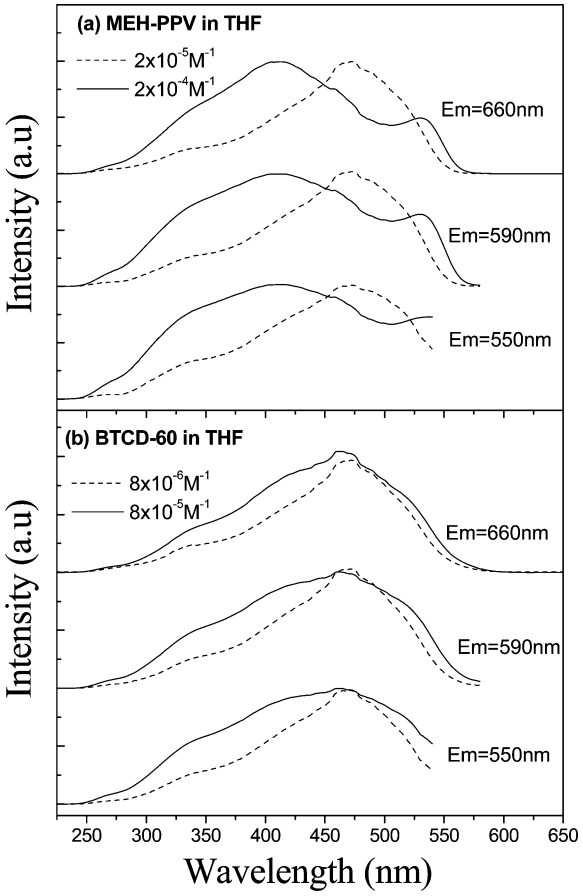

Figure 3. Excitation spectra of MEH-PPV (a) and BTCD-60 (b) in THF at different concentrations.

Solvent Induced π-Aggregation. In poly(phenylenevinylene)s, the polymer chains have a very strong affinity toward π-stacking, and the resultant π-aggregates in solution or solid state strongly quench the luminescence intensity.[29,30] In the present investigation, we have noticed that the introduction of bulky chains enhances the solution quantum yield as well as the PL intensity for both polymers as well as oligomers. Therefore, tracing the π-stacking properties of conjugated polymers, especially in the case of bulky systems, it is very important in understanding their luminescent properties. Solvent induced self-organization in conjugated chains is an attractive approach for this purpose since the isolation or aggregation of polymer chains can be easily controlled by choosing the appropriate combination of a good solvent or non-solvent (or bad solvent).[36] In a good solvent, the polymer chains exist as isolated chains, and subsequent addition of a bad solvent forces the polymer chains to enter a collapsed stage that is similar to that in the film. Therefore, solvent induced aggregation studies of the oligomers (MEH-OPV and BTCD-OPV) and polymers (BTCD-60 and MEH-PPV) will provide more insight into the effect of π-aggregation on the luminescent properties. For the solvent induced aggregation studies, the photophysical properties of polymers were studied in a THF (good solvent) and methanol (poor solvent) solvent mixture (THF and toluene were not promising). For the molecular aggregation studies of the model compounds, THF and water was chosen as the solvent combination. The absorption and emission spectra of MEH-PPV, BTCD-60, and BTCD-OPV in the THF/methanol (or THF/water) mixture (from 0 to 100% v/v) are shown in Figure 4 (the plots

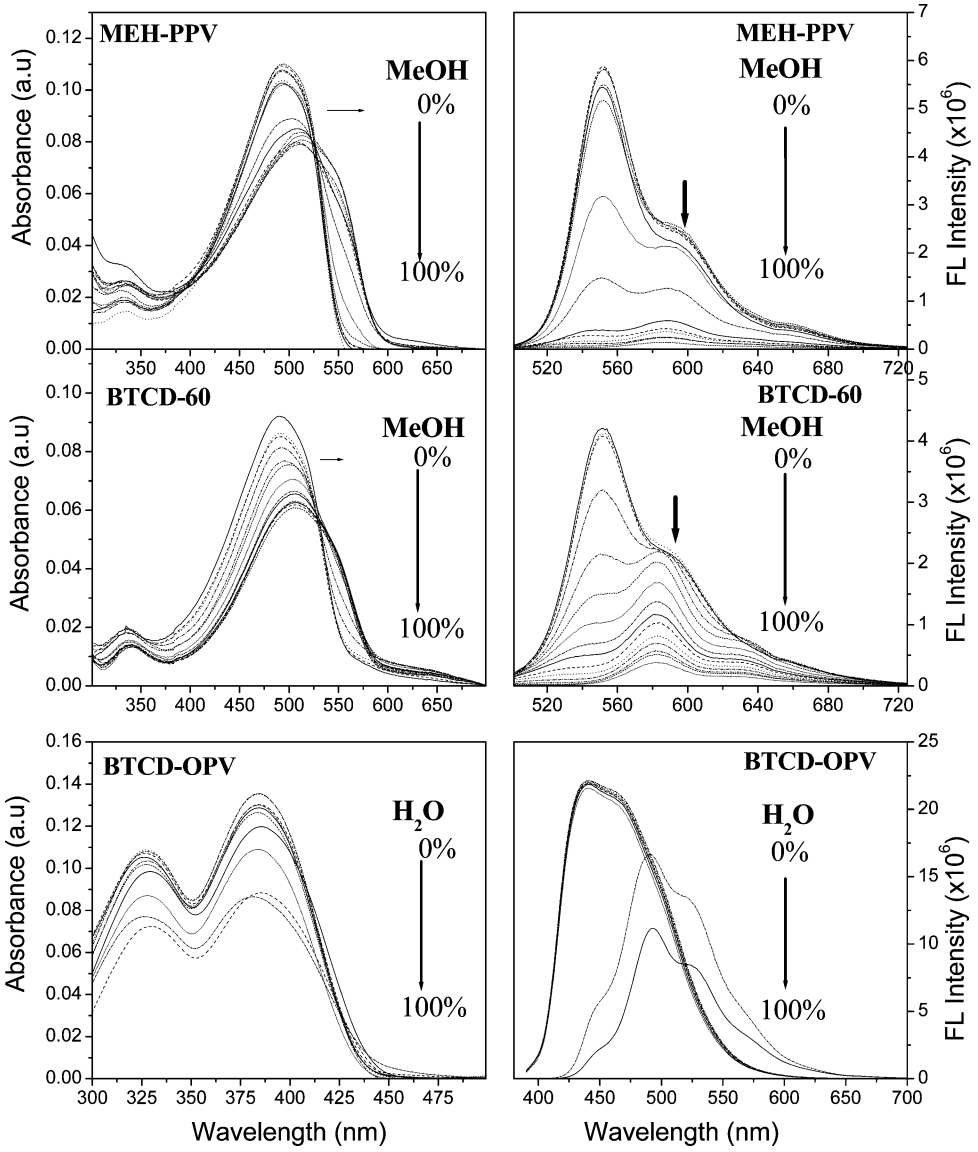

Figure 4. Absorption and emission spectra of polymers and OPVs in THF/MeOH or THF/H_2O with varying solvent combination at 30 °C.

for MEH-OPV are provided in the Supporting Information). The addition of methanol into the polymer solutions in THF drastically affect both the absorption maxima as well as the luminescent intensity. The color of the polymer solution gradually changed from orange to red with the addition of methanol, and the transition point was noted at 40−50% methanol in THF (see the images of vials in the Supporting Information). It can be clearly noticed that MEH-PPV was more drastically affected by the MeOH addition as compared to that of BTCD-60. The quantum yields for the solvent/non-solvent combinations were calculated using rhodamine 6G in water as the standard. Since the MeOH addition reflects both the absorption maxima and the quantum yield, these two parameters can be used to trace the extent of molecular aggregation in polymer chains. The plots of absorption maxima (Figure 5a) indicate the existence of two types of species depending upon the amount of methanol in the polymer solution. The polymer chains are free and isolated below 30−40% methanol, whereas they are fully aggregated above 50−60% methanol. The extent of absorption maxima shift (*Y*-axis) revealed that the MEH-PPV chains showed strong aggregation with a 25 nm red shift as compared to that of bulky BTCD-60, which showed only a 16 nm red shift. The quantum yield plots (Figure 5b) also support the existence of the aggregated chains, and the values are lower for MEH-PPV as compared to that of BTCD-60 (above 50% methanol concentration). This reveals that polymer chains in MEH-PPV chains experience more π-aggregation as compared to that of the bulky PPV chains in BTCD-60. The solvent induced aggregation studies of the model compounds (OPVs) also reflect the molecular aggregation in absorption and emission properties (see Figures 4 and 5c). As expected, the extent of aggregation is relatively weak in model compounds as compared to their polymer counterparts since long range π-stacking is not possible in simple OPVs as compared to that of high molecular weight polymer chains. The quantum yields of the model compound (Figure 5c) were almost unaffected up to 80% water in THF. However, at a higher water content, a significant decrease in quantum yield was noted for MEH-OPV as compared to that of BTCD-OPV. On the basis of the solvent induced aggregation studies, it can be concluded that the bulky TCD− unit is a very efficient anchoring group for the PPV backbone (also for OPVs) in preventing the molecular aggregation for enhanced emission properties.

Temperature Dependent Aggregation Studies. The aggregation of the polymer chains in solution is also sensitive to the temperature, which can also be used as another stimuli for tracing the molecular aggregation properties.[36] To study the influence of temperature on the nature and reversibility of the

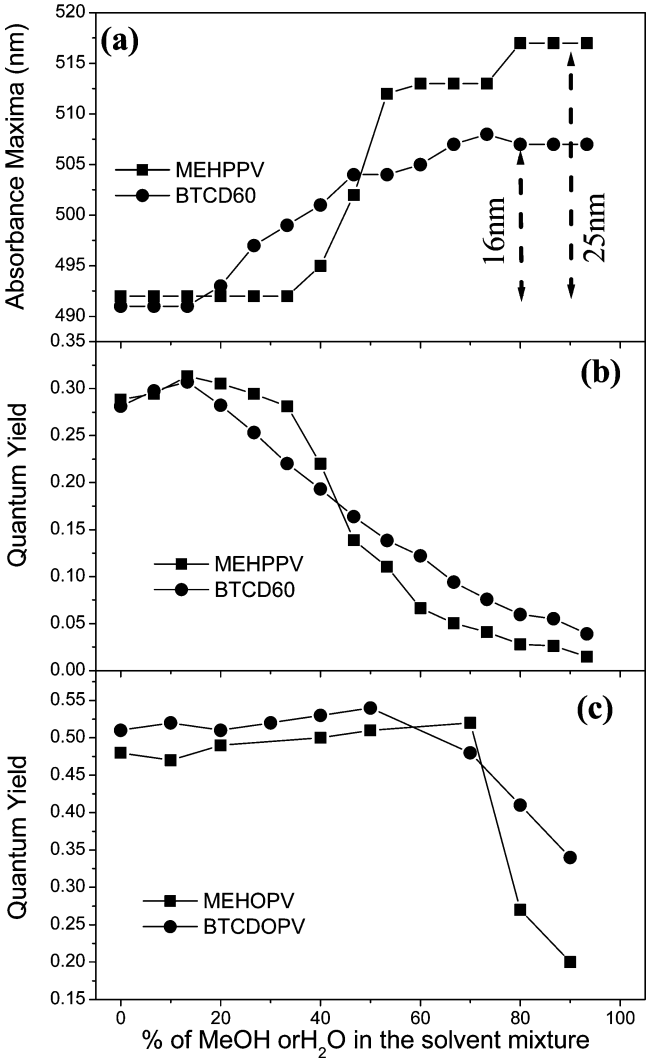

Figure 5. Plot of absorption maxima (a) and quantum yield (b and c) vs the percentage of MeOH or H_2O in the THF/MeOH or THF/MeOH mixture.

molecular aggregation in PPV chains, the polymers at the aggregated stage were subjected to temperature dependent absorption studies. There are two ways one can design the temperature dependent studies: (i) begin from the non-aggregated stage at room temperature and force the chains to undergo aggregation and isolation by cooling/heating at the subambient region[36] or (ii) begin from the pre-aggregated stage at room temperature and carry out the aggregation and isolation by heating/cooling at elevated temperatures. We adapted the second method because it is more relevant to practical purposes. For the temperature dependent studies, the 40% methanol in THF solvent combination was selected because at this stage, the polymers show a transition from the isolated to the aggregated state (see Figure 5a). The polymer solution (40% methanol in THF) was placed in a screw capped cuvette and subjected to absorption studies by heating or cooling the solution from 30 to 80 °C. The UV−vis spectra of BTCD-60 in the heating and cooling cycles are shown in Figure 6 (the spectra for MEH-PPV are given in the Supporting Information). As the solution temperature gradually increases, the absorption spectra were found to be blue shifted, corresponding to the isolation of polymer chains from the pre-aggregated state (see Figure 6b). While cooling, the absorbance spectra were red shifted, corresponding to the aggregation of polymer chains (see Figure 6a). This experiment was found to be completely reversible for many more heating/cooling cycles (see Supporting Information), which confirmed the reversibility of molecular aggregation in PPV chains. The shifts in the absorption maxima for the cooling and heating experiments are plotted and shown in Figure 6c,d, respectively. The absorption maxima plots indicated that the MEH-PPV chains underwent a 10 nm blue shift on heating, while 15 nm red shift in the cooling cycle occurred. The polymer chains in BTCD-60 followed just the opposite trend in the extent of the absorption maxima shift: they showed 14 nm blue shifts with heating and 10 nm red shifts in the cooling cycle. This trend suggests that both the polymers underwent isolation from the aggregated state, while for heating, however, the degree of interchain separation was higher for BTCD-60 (14 nm) as compared to MEH-PPV (10 nm). In the cooling cycle, the trend was found to be just the opposite, in which the MEH-PPV chains underwent more aggregation (15 nm) as compared to that of BTCD-60 (10 nm). The difference in the extent of aggregation from the isolated stage (in the cooling cycle) revealed that the bulky TCD units in the PPV− chains strongly hinder the polymer chain alignment and reduce the molecular aggregation. The results of temperature dependent studies are in accordance with the solvent induced aggregation studies where the interchain separations in the bulky systems reduced the molecular aggregation and enhanced the luminescent properties.

Polymer-Oligomer Binary Blends. To study the effect of bulky units on the interchain separation of PPV backbones, the MEH-PPV polymer was blended with MEH-OPV and BTCD-OPV through solution blending techniques. The two series of the blends were named MEH blend and BTCD blend, depending upon the types of OPV used in the blend preparation. The weight % of the oligomer was varied as 15, 30, 40, 55, 65, 80, 90, and 95% in the blend by varying the amount of the components. The blend solution was cast on a glass substrate in such a way as to maintain the optical density of the resultant film as ∼0.1. Two types of selective photophysical experiments can be carried out in the polymer-oligomer binary blend, which is explained in Figure 7: (i) selectively excite the oligomer and transfer the excitation energy to the polymer and subsequently monitor the emission of the polymer (energy transfer mechanism, path 1) or (ii) directly excite the polymer chains and monitor the polymer emission (path 2). In the case of path 1, the excitation of the OPV may also show self-emission, if the energy transfer process has failed. The efficiency of the energy transfer process in such binary blends is highly dependent on the energy levels of the molecules. To find the energy levels of the oligomers and polymers, redox behavior was studied using CV with a three electrode cell setup using 0.10 M Bu_4NPF_6 as the supporting electrolyte. The CV data for the polymer and oligomers are given in Table −1 (see plots in the Supporting Information). The electrochemical studies confirmed that the onset of the oxidation potential for the oligomers (0.93 V) was almost double as compared to that of the MEH-PPV polymer (0.52 V). The oxidation and reduction potential obtained matching that of the reported values.[69,70] The energy levels of the polymer and oligomers and the processes of paths 1 and 2 are shown in Figure 7. The absorption and emission spectra of the MEH and BTCD binary blends are shown in Figure 8. The absorption maxima of the OPV and PPV chains appeared at 390 and 500 nm, respectively. It is very clear from the plots that the optical densities of the PPV part increase with an increase in the MEH-PPV content in the blend. The emission spectra for 390 nm excitation (corresponding to the absorption maximum of the oligomer) are given in Figure 8c,d for the MEH and BTCD blends, respectively. In both blends, the emission spectra showed

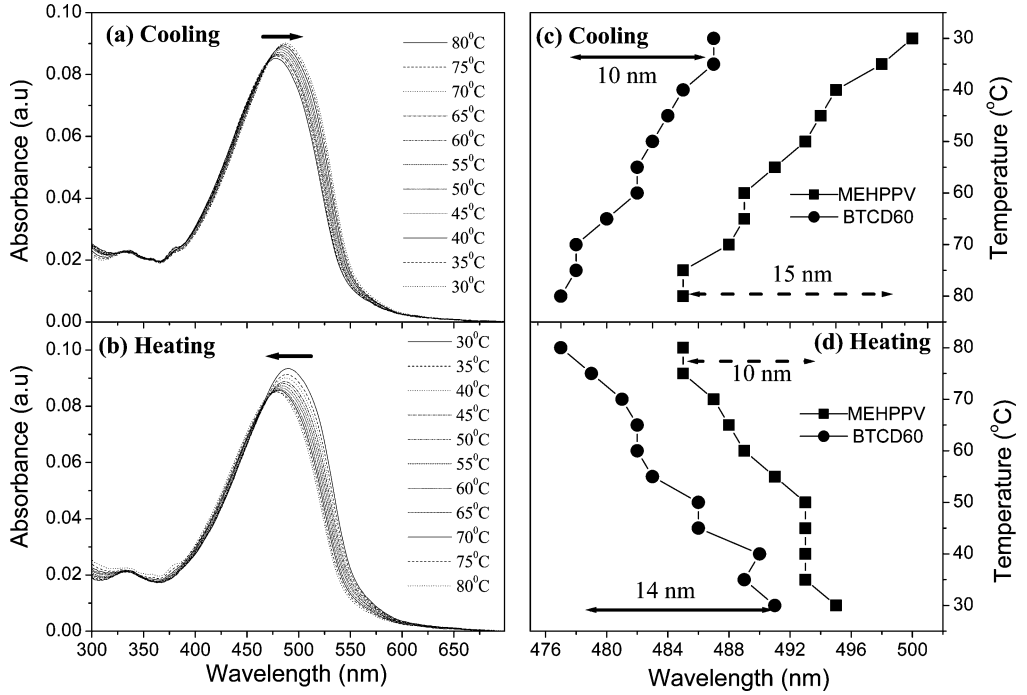

Figure 6. Temperature dependent absorption spectra (a and b) of BTCD-60 and plots of absorption maxima vs temperature for MEH-PPV and BTCD-60 in the cooling (c) and heating (d) cycles.

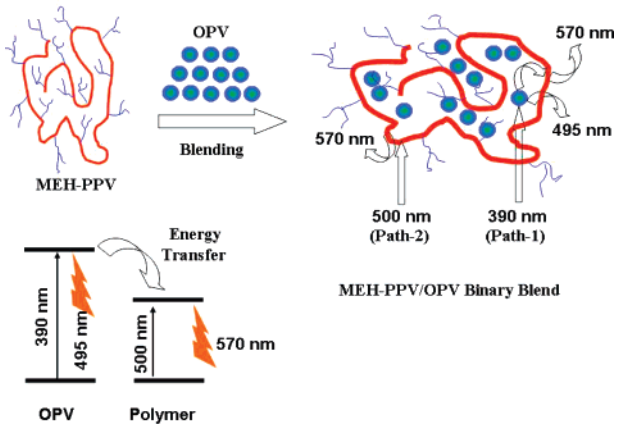

Figure 7. Polymer-oligomer binary blend and possible selective excitation processes in the blend.

two peaks at 495 and 570 nm corresponding to the self-emission and polymer chain emission followed by the energy transfer process, respectively. Pure MEH-PPV possess a small absorption at 390 nm (OD = 0.05, see Figure 8a,b) but failed to show any significant luminescence at 450−550 nm for excitation at 390 nm, which suggested that the pure MEH-PPV chains do not contribute to the emission characteristics of blends in this region. Therefore, the emission peaks at 495 and 570 nm in the blends are the result of the self-luminescence of OPVs and the emission of PPV chains followed by the energy transfer process from oligomer to polymer, respectively. The relative intensities of these emission peaks were highly influenced by the compositions and types of the OPVs in the blend. The emission intensities of the peaks at 495 and 570 nm were plotted with respect to their composition and are shown in Figure 9. It is very clear from the plots in Figure 9a that the MEH blend did not show self-luminescence up to 80% MEH-OPV content, which indicates a strong excitation energy transfer from the OPVs to the MEH-PPV chains. On the other hand, BTCD-OPV showed self-emission even for 30% of its presence in the BTCD blend. Figure 9b shows the luminescence intensities of the blend at 570 nm, followed by the energy transfer process from oligomer to polymer for 390 nm excitation. The energy transfer to the polymer chains leads to the luminescence of MEH-PPV at 570 nm. The increase in the PL intensity of the MEH-PPV chain was very high for the BTCD blend series throughout the entire composition (see Figure 9b); this suggests that the bulky OPV molecule showed an enhanced energy transfer process as compared to that of the normal OPV molecules. The emission spectra of the blends excited at 500 nm (with respect to the absorbance of MEH-PPV, path 2) are shown in Figure 8e,f, and the PL intensity data are plotted in Figure 9c. For 500 nm excitation, the blends showed an emission peak at 570 nm, and the intensity of this emission peak significantly increased with the amount of OPV in the blend (see Figure 9c) as compared to that of the pure MEH-PPV film. Since the OPV molecules do not have any luminescence behavior for excitation at 500 nm, the enhanced emission at 570 nm in the MEH-PPV chains is the result of the reduction of molecular aggregation in the solid state. The larger PL intensities of the BTCD blend at the entire composition indicate that the MEH-PPV polymer chains are separated apart very effectively by the BTCD-OPV molecules in the blend as compared to the MEH-OPVs. The well-separated polymer chains in the blend experience less π-stacking induced molecular aggregation. Therefore, it is directly evident from the selective excitation studies of the blends that the BTCD units are an efficient bulky group for controlling molecular aggregation for enhanced luminescence properties.

Time-Resolved Fluorescence Lifetime Measurements. Time-resolved fluorescence decay profiles of the polymers, oligomers, and polymer-oligomer blends were carried out in solution (THF) and in the film at room temperature. The decay dynamics was carried out at an excitation wavelength of 401 nm, and the decays were monitored at the respective emission maxima (see Table 2 and Figure 10). The OPVs in THF showed a single-exponential fit, and they possessed similar decay lifetimes, 1.86 ns (MEH-OPV) and 1.89 ns (BTCD-OPV), indicating that they have similar excimer species.[22,64] The decay profiles of MEH-OPV and BTCD-OPV in film were found to be similar to that

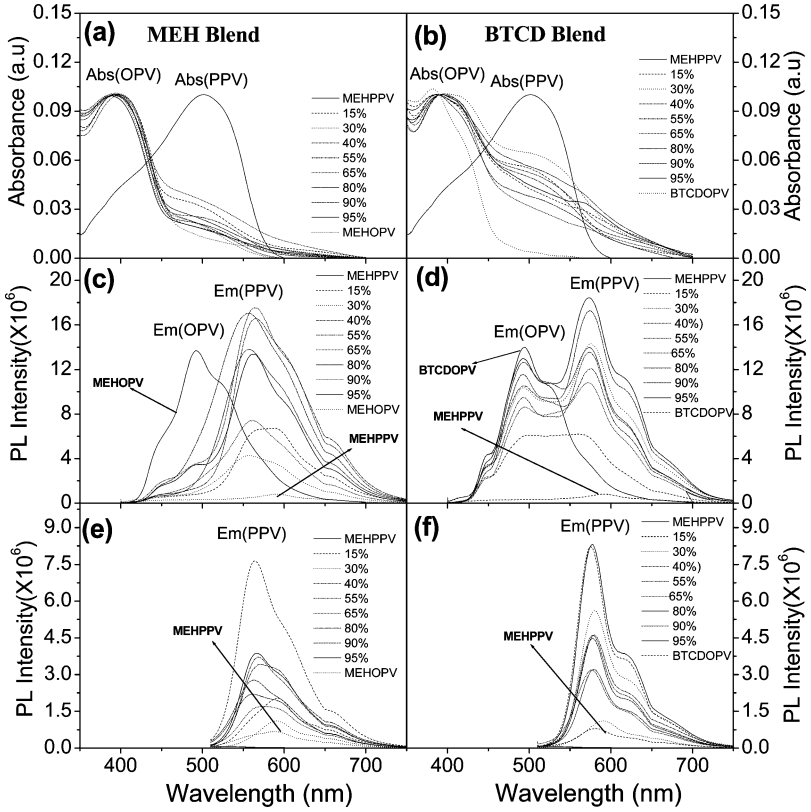

Figure 8. Absorption spectra of MEH blend (a) and BTCD blend (b). Emission spectra of MEH blend for excitation wavelengths 390 nm (c) and 500 nm (e). Emission spectra of BTCD blend for excitation wavelengths 390 nm (d) and 500 nm (f).

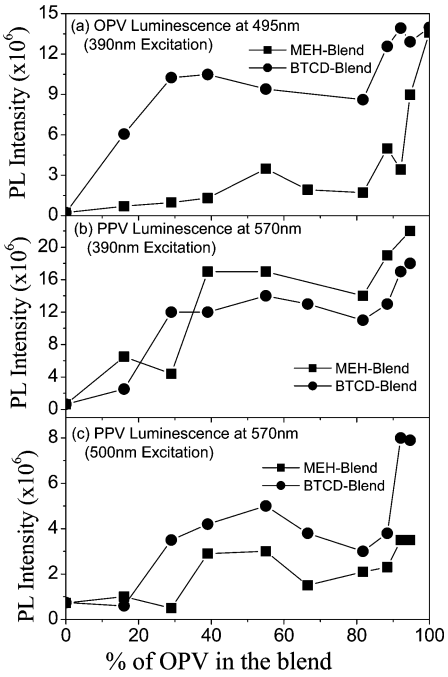

Figure 9. Plot of PL intensity vs % OPV (a) in the blend for MEH blend and BTCD blend at different excitation wavelengths (b and c).

in solution. MEH-PPV and BTCD-60 showed a single-exponential decay in THF with a lifetime of 0.56−0.60 ns. The aggregated polymer solution (40% methanol in THF) showed biexponential decay with two lifetimes in the range of 0.50−0.60 ns (98%) and 0.81−1.04 ns (2%), confirming the existence of two types of luminescent species corresponding to the aggregated and isolated chains. The polymers in film also showed a biexponential decay, and their lifetimes are given in Table 2. The observed fast decay in the aggregated solution

TABLE 2: Fluorescent Decay Lifetime Measurements of Oligomers, Polymers, and Polymer-Oligomer Blends

sample	medium[a]	$\lambda_{monitor}$ (nm)[b]	τ_1 (ns)[c] (99%)	τ_2 (ns)[c] (1%)
MEH-OPV	THF	470	1.86	
BTCD-OPV	THF	470	1.89	
MEH-OPV	film	525	1.70	
BTCD-OPV	film	525	2.04	
MEH-PPV	THF	555	0.56	
BTCD-60	THF	555	0.60	
MEHPPV-Agg	THF/CH_3OH	550	0.50	1.04
BTCD60-Agg	THF/CH_3OH	550	0.61	0.81
MEH-PPV	film	585	0.46	0.62
BTCD-60	film	585	0.35	0.56
MEHBlend-30	film	585	0.52	1.17
MEHBlend-90	film	585	0.34	0.81
BTCDBlend-30	film	575	0.32	1.33
BTCDBlend-90	film	575	0.36	1.69
BTCDBlend-30	film	495	0.63	2.46
BTCDBlend-90	film	495	0.51	2.35

[a] Optical density of solutions and films was maintained at ≈0.1 for the lifetime measurements. [b] Emission wavelengths for which the decay was monitored (λ_{exc} = 401 nm). [c] Lifetimes obtained from the exponential decay fitting.

and in the films may be due to the increased extent of nonradiative processes and efficient energy transfer to the aggregated species. The decay lifetime measurements of the polymer-oligomer binary blends were also carried out in films, and they showed a biexponential fit (Figure 10d). It was clear from the fitting results that more than 90% of the components underwent a fast decay and that only less than 10% showed a delayed emission. In the MEH blend, as the percentage of OPV in the blend increased, the decay lifetime became fast because of the high rate of the energy transfer process from the oligomer to the polymer chain. This observation in the MEH blend demonstrated complete energy transfer from the oligomer, which

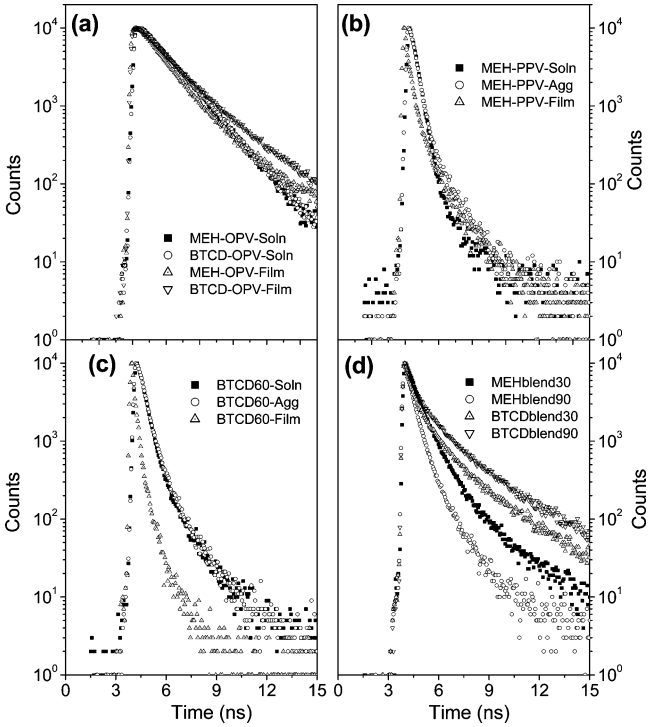

Figure 10. Fluorescence lifetime decay curves of OPVs, PPVs, and their blends in solution and film (a−d).

resulted in the increase in emission intensity of the polymer. However, the decay lifetime of the BTCD blend showed no difference for the emission wavelength collected at 575 nm, which corresponded to the polymer emission. But, a small difference was observed for the BTCD blend films when collected at 495 nm, which corresponds to the oligomer emission. This supports the observation for the polymer-oligomer binary blends that in the BTCD blend, two significant processes occur: (i) the self-luminescence of the oligomer and (ii) the emission of the polymer chains as a result of the enhanced energy transfer. It is evident that the bulky OPV sterically hinders the interchain interactions, preventing molecular aggregation in the solid state. Therefore, from photophysical studies and decay lifetime measurements, it can be concluded that the bulky TCD− unit is an important anchoring group, which can control molecular aggregation by increasing the interchain distances in the polymer chains as well as in the polymer-oligomer blend for the enhanced luminescence properties.

Conclusion

In conclusion, we demonstrated the importance of the bulky TCD anchoring group in controlling molecular aggregation for improving photoluminescence properties. The absorption, excitation, and emission studies of the polymers in solution and solid state demonstrated that apart from the solvent effects, the structural configuration of the polymeric backbone plays an important role in enhancing the solid-state luminescence intensity. The presence of a TCD bulky unit in BTCD-60 significantly hindered the π-stacking of the polymer backbone and enhanced the solid-state luminescence almost 5−6 times as compared to that of MEH-PPV. The solvent induced and temperature dependent aggregation studies in solution confirmed the importance of the bulky unit in controlling the molecular aggregation in the PPV backbone. The photophysical studies of the polymer-oligomer blend revealed that the bulky OPV (BTCD-OPV) increased the emission of the PPV chain via both energy transfer and interchain separation processes. Decay lifetime measurements of the binary blends further support efficient energy transfer from the OPV to the PPV backbone, resulting in enhanced emission properties. From the present investigation, it was clearly evident that the bulky substitution in the PPV or in the oligomer separates the interchain or intermolecular distance more efficiently, leading to improved photoluminescence properties that can be explored for the futuristic applications of optoelectronic devices.

Acknowledgment. We thank KSCTSE, Thiruvananthapuram, Kerala, India (082/SRSPS/2004/CSTE) for financial support. S.R.A. thanks CSIR-New Delhi, India for a research fellowship. We greatly acknowledge Celanese Chemicals Ltd. for providing TCD research samples.

Supporting Information Available: Procedure for preparation of polymer-oligomer blends, DSC plots, aggregation studies of MEH-OPV, temperature dependent aggregation studies of MEH-PPV, reversibility of aggregation in polymers, and cyclic voltammogram of OPVs and PPVs. This information is available free of charge via the Internet at http://pubs.acs.org.

References and Notes

(1) Akcelrud, L. *Prog. Polym. Sci*. **2003**, *28*, 875.
(2) Burroughes, J. H.; Bradley, D. D. C.; Brown, A. R.; Marks, R. N.; Mackay, K.; Friend, R. H.; Burns, P. L.; Holmes, A. B. *Nature (London, U.K.)* **1990**, *347*, 539.
(3) Friend, R. H.; Gymer, R. W.; Holmes, A. B.; Burrouges, J. H.; Marks, R. N.; Taliani, C.; Bradley, D. D. C.; dos Santos, D. A.; Gredas, J. L.; Longlund, M.; Salaneck, W. R. *Nature (London, U.K.)* **1999**, *397*, 121.
(4) Sheats, J. R.; Antoniadis, H.; Hueschen, M.; Leonard, W.; Miller, J.; Moon, R.; Roitman, D.; Stocking, A. *Science (Washington, DC, U.S.)* **1996**, *273*, 884.
(5) Kraft, A.; Grimsdale, A. C.; Holmes, A. B. *Angew. Chem., Int. Ed.* **1998**, *37*, 402.
(6) Lidzey, D. G.; Bradley, D. D. C.; Alvarado, S. F.; Seidler, P. F. *Nature (London, U.K.)* **1997**, *386*, 135.
(7) Egbe, D. A. M.; Tillmann, H.; Rirckner, E.; Klemm, E. *Macromol. Chem. Phys.* **2001**, *202*, 2712.
(8) Samuel, I. D. W.; Rumbles, G.; Collison, C. J.; Moratti, S. C.; Holmes, A. B. *Chem. Phys.* **1998**, *227*, 75.
(9) Zou, Y.; Hou, J.; Yang, C.; Li, Y. *Macromolecules* **2006**, *39*, 8889.
(10) Fan, Q. L.; Lu, S.; Lai, Y. H.; Hou, X. Y.; Huang, W. *Macromolecules* **2003**, *36*, 6976.
(11) Ahn, T.; Song, S. Y.; Shim, H. K. *Macromolecules* **2000**, *33*, 6764.
(12) Sun, H.; Mei, C.; Zhou, Q.; Liu, Z.; Ma, D.; Wang, L.; Jing, X.; Wang, F. *J. Polym. Sci., Part A: Polym. Chem.* **2006**, *44*, 3469.
(13) Ahn, T.; Ko, S. W.; Lee, J.; Shim, H. K. *Macromolecules* **2002**, *35*, 3495.
(14) Patil, A. O.; Heeger, A. J.; Wudl, F. *Chem. Rev.* **1988**, *88*, 183.
(15) Li, X. G.; Huang, M. R.; Duan, W.; Yang, Y. L. *Chem. Rev.* **2002**, *102*, 2925.
(16) Anderson, M. R.; Mattes, B. R.; Reiss, H.; Kaner, R. B. *Science (Washington, DC, U.S.)* **1991**, *252*, 1412.
(17) Huang, M. R.; Li, X. G.; Yang, Y. L.; Wang, X. S.; Yan, D. *J. Appl. Polym. Sci*. **2001**, *81*, 1838.
(18) Li, X. G.; Wei, F.; Huang, M. R.; Xie, Y. B. *J. Phys. Chem. B* **2007**, *111*, 5829.
(19) Lu, Q. F.; Huang, M. R.; Li, X. G. *Chem.—Eur. J.* **2007**, *13*, 6009.
(20) MacDiarmid, A. G. *Angew. Chem., Int. Ed.* **2001**, *40*, 2581.
(21) Traiphol, R.; Charoenthai, N.; Srikhirin, T.; Kerdcharoen, T.; Osotchan, T.; Maturos, T. *Polymer* **2007**, *48*, 813.
(22) Hsu, J. H.; Fann, W.; Tsao, P. H.; Chuang, K. R.; Chen, S. A. *J. Phys. Chem. A* **1999**, *103*, 2375.
(23) Jakubiak, R.; Collison, C. J.; Wan, W. C.; Rothberg, L. J.; Hsieh, B. R. *J. Phys. Chem. A* **1999**, *103*, 2394.
(24) Chen, S. H.; Su, A. C.; Chou, H. L.; Peng K. Y.; Chen, S. A. *Macromolecules* **2004**, *37*, 167.
(25) Huang, W. Y.; Matsuoka, S.; Kwei, T. K.; Okamoto, Y. *Macromolecules* **2001**, *34*, 7166.
(26) Setayesh, S.; Grimsdale, A. C.; Weil, T.; Enkelmann, V.; Mullen, K.; Meghdadi, F.; List, E. J. W.; Leising, G. *J. Am. Chem. Soc.* **2001**, *123*, 946.
(27) Bunz, U. H. F. *Chem. Rev.* **2000**, *100*, 1605.

(28) Becker, H.; Spreitzer, H.; Kreuder, W.; Kluge, E.; Schenk, H.; Parker, I.; Cao, Y. *Adv. Mater*. **2000**, *12*, 42.
(29) Shi, Y.; Liu, J.; Yang, Y. *J. Appl. Phys*. **2000**, *87*, 4254.
(30) Nguyen, T. Q.; Doan, V.; Schwartz, B. J. J. *Chem. Phys*. **1999**, *110*, 4068.
(31) Padmanabhan, G.; Ramakrishnan, S. *J. Am. Chem. Soc*. **2000**, *122*, 2244.
(32) Liao, L.; Pang, Y.; Ding, L.; Karasz, F. E.; Smith, P. R.; Meador, M. A. *J. Polym. Sci., Polym. Chem.* **2004**, *42*, 5853.
(33) (a) Liao, L.; Pang, Y.; Ding, L.; Karasz, F. E. *Macromolecules* **2002**, *35*, 3819. (b) Pang, Y.; Li, J.; Hu, B.; Karasz, F. E. *Macromolecules* **1999**, *32*, 3946.
(34) Liao, L.; Pang, Y.; Ding, L.; Karasz, F. E. *Macromolecules* **2001**, *34*, 6756.
(35) Zheng, M.; Sarker, A. M.; Gurel, E. E.; Lahti, P. M.; Karaz, F. E. *Macromolecules* **2000**, *33*, 7426.
(36) (a) Chu, Q.; Pang, Y. *Macromolecules* **2003**, *36*, 4614. (b) Chu, Q.; Pang, Y. *Macromolecules* **2005**, *38*, 517.
(37) Marchioni, F.; Chiechi, R.; Patil, S.; Wudl, F.; Chen, Y.; Shinar, J. *Appl. Phys. Lett.* **2006**, *89*, 61101.
(38) Lee, J. I.; Kang, I. N.; Hwang, D. H.; Shim, H. K. *Chem. Mater*. **1996**, *8*, 1925.
(39) Peng, K. Y.; Chen, S. A.; Fann, W. S. *J. Am. Chem. Soc*. **2001**, *123*, 11388.
(40) Alam, M. M.; Jenekhe, S. A. *Macromol. Rapid Commun*. **2006**, *27*, 2053.
(41) (a) Chou, C. H.; Hsu, S. L.; Dinakaran, K.; Chiu, M. Y.; Wei, K. H. *Macromolecules* **2005**, *38*, 745. (b) Xia, C.; Advincula, R. C. *Macromolecules* **2001**, *34*, 5854.
(42) (a) Yang, J. S.; Swager, T. M. *J. Am. Chem. Soc*. **1998**, *120*, 5321. (b) Yang, J. S.; Swager, T. M. *J. Am. Chem. Soc*. **1998**, *120*, 11864.
(43) Wang, H.; Song, N.; Li, H.; Li, Y.; Li, X. *Synth. Met*. **2005**, *151*, 279.
(44) Tang, R.; Chuai, Y.; Cheng, C.; Xi, F.; Zou, D. *J. Polym. Sci., Part A: Polym. Chem*. **2005**, *43*, 3126.
(45) Bao, Z.; Amundson, K. R.; Lovinger, A. J. *Macromolecules* **1998**, *31*, 8647.
(46) Ko, S. W.; Jung, B. J.; Cho, N. S.; Shim, H. K. *Bull. Korean Chem. Soc*. **2002**, *23*, 1235.
(47) Choo, D. J.; Talaie, A.; Lee, Y. K.; Jang, J.; Park, S. H.; Huh, G.; Yoo, K. H.; Lee, J. Y. *Thin Solid Films* **2000**, *363*, 37.
(48) Jeong, H. Y.; Lee, Y. K.; Talaie, A.; Kim, K. M.; Kwon, Y. D.; Jang, Y. R.; Yoo, K. H.; Choo, D. J.; Jang, J. *Thin Solid Films* **2002**, *417*, 171.
(49) Lee, Y. K.; Jeong, H. Y.; Kim, K. M.; Kim, J. C; Choi, H. Y.; Kwon, Y. D.; Choo, D. J.; Jang, Y. R.; Yoo, K. H.; Jang, J.; Talaie, A. *Curr. Appl. Phys.* **2002**, *2*, 241.
(50) Anderson, M. R.; Yu, G.; Heeger, A. J. *Synth. Met.* **1997**, *85*, 1275.
(51) Wudl, F.; Hoger, S.; Zhang, C.; Pakbaz, K.; Heeger, A. J. *Polym. Prepr*. **1993**, *34*, 197.
(52) (a) Mikroyannidis, J. A. *Macromolecules* **2002**, *35*, 9289. (b) Spiliopoulos, I. K.; Mikroyannidis, J. A. *Macromolecules* **2002**, *35*, 2149. (c) Spreitzer, H.; Becker, H.; Kluge, E.; Kreuder, W.; Schenk, H.; Demandt, R.; Schoo, H. *Adv. Mater*. **1998**, *10*, 1340. (d) Johansson, D. M.; Srdanov, G.; Yu, G.; Theander, M.; Inganas, O.; Andersson, M. R. *Macromolecules* **2000**, *33*, 2525. (e) Hsieh, B. R.; Yu, Y.; Forsythe, E. W.; Schaaf, G. M.; Feld, W. A. *J. Am. Chem. Soc.* **1998**, *120*, 231. (f) Wan, W. C.; Antoniadis, H.; Choong, V. E.; Razafitrimo, H.; Gao, Y.; Feld, W. A.; Hseih, B. R. *Macromolecules* **1997**, *30*, 6567. (g) Lee, S. H.; Jang, B. B.; Tsutsui, T. *Macromolecules* **2002**, *35*, 1356. (h) Chen, Z. K.; Lee, N. H. S.; Huang, W.; Xu, Y. S.; Cao, Y. *Macromolecules* **2003**, *36*, 1009.
(53) Sarker, A. M.; Ding, L.; Lahti, P. M.; Karasz, F. E. *Macromolecules* **2002**, *35*, 223.
(54) Lee, N. H. S.; Chen, Z. K.; Huang, W.; Xu, Y. S.; Cao, Y. *J. Polym. Sci., Part A: Polym. Chem.* **2004**, *42*, 1647.
(55) Chen, Z. K.; Wang, L. H.; Kang, E. T.; Huang, W. *Phys. Chem. Chem. Phys*. **1999**, *1*, 3789.
(56) Chou, C. H.; Hsu, S. L.; Yeh, S. W.; Wang, H. S.; Wei, K. H. *Macromolecules* **2005**, *38*, 9117.
(57) Xiao, S.; Nguyen, M.; Gong, X.; Cao, Y.; Wu, H.; Moses, D.; Heeger, A. J. *Adv. Funct. Mater*. **2003**, *13*, 25.
(58) Tokito, S.; Tanaka, H.; Noda, K.; Okada, A.; Taga, Y. *Appl. Phys. Lett*. **1997**, *70*, 1929.
(59) Amrutha, S. R.; Jayakannan, M. *J. Phys. Chem. B* **2006**, *110*, 4083.
(60) Amrutha, S. R.; Jayakannan, M. *Macromolecules* **2007**, *40*, 2380.
(61) (a) Wang, L. X.; Li, X. G.; Yang, Y. L. *React. Funct. Polym*. **2001**, *47*, 125. (b) Matthews, J. R.; Goldoni, F.; Schenning, A. P. H. J.; Meijer, E. W. *Chem. Commun*. **2005**, 5503.
(62) Traiphol, R.; Sanguansat, P.; Srikhirin, T.; Kerdcharoen, T.; Osotchan, T. *Macromolecules* **2006**, *39*, 1165.
(63) Ding, L.; Egbe, D. A. M.; Karasz, F. E. *Macromolecules* **2004**, *37*, 6124.
(64) Fakis, M.; Anestopoulos, D.; Giannetas, V.; Persephonis, P. *J. Phys. Chem. B* **2006**, *110*, 24897.
(65) Bril, A.; De Jager-Veenis, A. W. *J. Electrochem. Soc.* **1976**, *123*, 396.
(66) Biju, S.; AmbiliRaj, D. B.; Reddy, M. L. P.; Kariuki, B. M. *Inorg. Chem*. **2006**, *45*, 10651.
(67) Fu, L.; Ferreira, R. A. S.; Silva, N. J. O.; Fernandes, A. J.; Ribeiro-Claro, P.; Goncalves, I. S.; Bermudez, V. Z.; Carlos, L. D. *J. Mater. Chem*. **2005**, *15*, 3117.
(68) Silva, F. R. G.; Menezes, J. F. S.; Rocha, G. B.; Alves, S.; Brito, H. F.; Longo, R. L.; Malta, O. L. *J. Alloy Compd.* **2000**, *303*−*304*, 364.
(69) Meng, H.; Yu, W. L.; Huang, W. *Macromolecules* **1999**, *32*, 8841.
(70) Xiao, Y.; Yu, W. L.; Pei, J.; Chen, Z.; Huang, W.; Heeger, A. J. *Synth. Met.* **1999**, *106*, 165.